SLAC-PUB-663
September 1969
(ACC)

MICROWAVE STUDIES AT THE STANFORD LINEAR ACCELERATOR CENTER*

H. A. Hogg

Stanford Linear Accelerator Center
Stanford University, Stanford, California 94305

I. INTRODUCTION

The fundamental role of microwave power at SLAC is to accelerate the electron beam along its two-mile course. The traveling wave acceleration of electrons in conventional machines has been extensively treated in the literature, however, and will not be discussed here. Nevertheless, there are some microwave problems and developments of recent origin, two of which will be described in this paper. The first concerns the limitation in the amount of current transmitted through the machine, caused by beam breakup: the second looks toward one form of the next generation of high energy physics machines, viz., the superconducting accelerator.

(1969 European Microwave Conference, London, Sept. 8-12, 1969)

---

*Work supported by the U. S. Atomic Energy Commission.

II. BEAM BREAKUP IN LINEAR ACCELERATORS

The unpalatable phenomenon of beam breakup was first reported in 1958, and has since been the object of intensive study by accelerator engineers – especially those concerned with the building of machines which are very long, or which operate at a high duty cycle.

The manifestation of beam breakup is a transverse oscillation of the electron beam which increases with current, pulse length and distance traveled along the accelerator, eventually resulting in loss of the beam to the walls of the disk-loaded slow-waveguide.

There are two breakup mechanisms, both based upon interaction with the "TM_{11}-like" HEM_{11} mode, which can propagate in the disk-loaded structure (Fig. 1). Normal electron acceleration is achieved by the TM_{01} mode, illustrated here for the SLAC design in which the phase velocity v_p is equal to c at $\beta d = 2\pi/3$. It can be seen that, for the same structure, a beam traveling with the velocity of light interacts with the HEM_{11} backward-wave near the π-mode. (The dispersion curves are multiplets because the slow-wave structure is designed to present the same accelerating field to the beam in every cavity, taking into account structure attenuation and 5% beam loading: thus no two cavities in a 10-foot accelerator section have the same dimensions.

The negative group velocity of the HEM_{11} mode can give rise to regenerative backward-wave oscillation within a single accelerator section, but the starting currents are high, and this form of beam breakup is not observed at SLAC. The second breakup mechanism, in which the beam cumulatively interacts with trapped HEM_{11} resonances in the first few cavities of successive accelerator sections, is illustrated in Fig. 2. Transverse noise modulation on the beam excites the resonance in accelerator sections following the injector. As a result, succeeding electron bunches receive additional transverse momentum which is translated into displacement modulation as the bunches pass down the accelerator. This modulation further excites the downstream cavities which, in turn, deflect the beam even more until it is intercepted by the accelerator walls. The asymptotic phase for maximum amplification is intermediate between the optimum phases for momentum transfer and field excitation.

Several analyses of cumulative beam breakup have been given. These have been reviewed by Helm and Loew.[1] A model based on various simplifying assumptions leads to a solution of the form

$$x(z,t) \approx x_0 \exp\left[\left\{CIt\left(\int_0^z \gamma^{-1/2}\, dz\right)^2\right\}^{1/3} - \omega_1 t/2Q\right]$$

where x is the transverse displacement of initial value x_0, Q is the quality factor of the HEM_{11} resonance at frequency $\omega_1/2\pi$, C is proportional to the shunt impedance divided by Q, I is the current, t is time, z is distance traveled, and γ is the normalized energy. The assumptions include (1) the region in each accelerator section in which the resonance occurs can be represented by a single cavity. (2) All these equivalent cavities resonate at the same frequency. (3) The breakup frequency is not a simple harmonic of the accelerator frequency. (4) The axial velocities of the electrons are relativistic. (5) No magnetic focusing is applied to the beam.

The simple analytical model has been extended by Panofsky[2] to include the effect of weak magnetic focusing. The predictions of this theory have been verified at SLAC under suitable focusing conditions.

To obtain accurate predictions of beam breakup in a long, multisection accelerator with strong focusing, it is necessary to resort to computer studies.

Helm[3] has done extensive calculations using a coupled-resonator model of the accelerator structure. The computer program permits ray-tracing of individual electron bunches through the two-mile machine, and takes into account the effects of axial acceleration, drift-spaces (sections with no acceleration), and discrete magnetic focusing lenses.

In parallel with the computer work, many microwave experiments have been carried out, both on the operating machine and on separate accelerator waveguide sections. For instance, low-Q microwave cavities designed to detect transverse oscillations in the electron beam in the horizontal and vertical planes were installed at intervals along the machine. These were used to measure beam oscillation frequencies and growth rates along the accelerator. Cavities near the injector have been externally excited at the breakup frequencies, to study starting mechanisms. Computed frequencies and field distributions for the first, second and third HEM_{11} modes are shown in Fig. 3b. These are in excellent agreement with perturbation measurements, and with resonances indicated by input VSWR peaks (Fig. 3a).

The first improvement in breakup current threshold was achieved during 1967 by rearranging the machine focusing system. Quadrupole singlets were installed every 40 feet along the beam line in the first six sectors (2000 feet) of the machine. The remainder of the machine was focused by quadrupole doublet lenses, placed at sector (333 feet) intervals. The increased focusing strength, particularly in the early sectors, dampened the growth of transverse oscillations on the beam and increased the breakup current threshold from 20 to 40 mA.

The second line of attack on the problem has been to shift the HEM_{11} resonant frequency in selected sectors of the machine, thus detuning and lowering the gain of the transverse-wave amplifier. The frequency is shifted by slightly deforming the three cavities in each 10-foot accelerator section which contain the maximum HEM_{11} fields. Deformation is effected by four hydraulically-actuated plungers which are forced into the outer wall of the cavity, "dimpling" the surface at four places equally spaced around the periphery. Various detuning patterns have been evaluated by computer calculations; basically the selected pattern amounts to detuning one third of the machine by 4 MHz, one third by 2 MHz and leaving the remainder untouched. When the three cavities in a section are dimpled sufficiently to produce a 4 MHz increase in the HEM_{11} resonant frequency, the transmission phase-shift for the TM_{01} accelerating mode (2856 MHz) is changed by about 27 degrees. In order to maintain a good input VSWR, the middle cavity has to be tuned more than the outer two.

All 4 MHz tuning has been done under the scrutiny of careful microwave monitoring of frequencies, phase-shift and VSWR. However, this process is tedious and slow, and involves some risk of contaminating the accelerator vacuum system, as the sector being tuned has to be let up to dry nitrogen, and all waveguide seals have to be broken. For this reason, the mechanical precision of the dimpling tool has been improved to the point at which the 2 MHz tuning can be accomplished without microwave measurements. This of course means that the accelerator vacuum system does not have to be disturbed. An attempt will be made to carry out the 4 MHz tuning by the same purely mechanical process.

So far, two sectors have been detuned by 4 MHz, and six by 2 MHz. This work has raised the breakup current threshold (for a 17 GeV beam) from 40 to 65 mA. The loss in energy due to phase rotation in the first five cavities of each section has been too small to measure.

III. SUPERCONDUCTING ACCELERATOR STUDIES

During the past year, a study program covering all aspects of building a very large superconducting linear accelerator has been started at SLAC. The impetus for this work derives from the need to upgrade the performance of the accelerator within the next decade to meet the anticipated future demands of high energy physics research. Adoption of a superconducting slow-wave structure with vanishingly small rf losses can theoretically result in striking improvements in accelerator performance. The present maximum beam energy at SLAC is a little over 20 GeV, and the beam current duty cycle is 0.06%: it is anticipated that a superconducting machine of the same length could raise these parameters to 100 GeV and 6%, respectively. The increase in energy would open a new realm of physics research, and the 100-fold increase in duty cycle would greatly improve experimental statistics.

At present, the preferred operating temperature of a superconducting accelerator is $1.85^{\circ}K$. Ultimately, the selection depends on the state of the art in the technologies of refrigeration and superconducting materials: if we can reliably produce and maintain structures with higher Q's by working at lower temperatures, then it may be more economical to design the refrigeration system to remove a smaller number of watts at a lower temperature. In any event, it is very advantageous to work below the lambda-point of liquid helium, to take advantage of the superfluid properties of Helium II. At $1.85^{\circ}K$, about 50% of the liquid is Helium II.

The superconducting accelerator must not only be a high-Q structure: it must maintain its low-loss characteristic at the very high microwave fields required to produce the specified beam acceleration. This obviously places additional requirements on superconductor performance, and it also means that the accelerator structure must be designed to maximize the ratios of axial accelerating field E_0 to the peak E and H fields occurring in the structure. Computer programs are being developed to study how, for a given surface impedance, the quantities Q, r_0 (shunt impedance), E_{peak}/E_0 and H_{peak}/E_0 vary with cavity shape and group velocity.

Concern with minimizing E_{peak}/E_0 has also led to the pro-tem adoption of a traveling-wave structure, which has a significantly lower ratio of peak to average fields than a standing-wave structure. At the end of the traveling-wave section, the residual power is coupled into a superconducting rectangular waveguide and fed back into the section input, forming a resonant ring. The arrangement is shown schematically in Fig. 4. The input coupler is designed so that, when the feedback phase in the loop is properly adjusted, the power input from the klystron exactly balances the losses in the loop due to beam loading and wall attenuation. Under these optimum conditions, no power flows into the load arm of the coupler, and the coupling ratio is equal to the ratio of the powers being combined. The tentative design at 2856 MHz assumes a klystron power of 20 kW, split to feed two resonant loops, so that 10 kW are incident upon each coupler. The coupling ratio is 37.37 dB, and the power circulating in the ring is 54.6 MW. The length of accelerator in each loop is 20 feet, and the accelerating field (based on achieving 100 GeV in 10,000 feet) is 10 MV per foot. Thus, at a beam current of 48 μA, 9.6 kW is extracted from the loop fields by the beam and 400 W is dissipated in the superconducting structure. Multiplying by the 6% duty factor, this amounts to 1.2 W/ft, which is the design capacity of the refrigeration system.

At energies below 100 GeV, the beam current may be increased as shown in Fig. 5, to maintain the optimum power ratio at the input coupler. In addition, the duty cycle may be raised without exceeding refrigeration capacity. (It is assumed that it will not be possible to operate above 100 GeV, because of the peak field limitations.)

It is apparent that the phasing and matching requirements in such a loop are formidable. It can be shown[4] that the fractional loss in beam energy due to an error of ϕ radians in loop phase closure is given by $\delta V/V = -(g\phi)^2$, where g is the coupling, expressed as a ratio (5.46×10^3 in the case being discussed). Thus, to avoid energy losses exceeding 1%, the loop phase must be maintained to within 1 millidegree. Furthermore, in a ring with the parameters presented here, a mismatch giving rise to a voltage reflection coefficient of 1×10^{-5} will reduce the accelerating fields by 1% and present a VSWR of 1.2 to the klystron.

For these reasons, servo-operated phasing and matching systems as illustrated in Fig. 4 are being designed. The loop phase is maintained by comparing the outputs of couplers C_2 and C_3 in a phase bridge, and using the detected error signal to drive tuning plungers in the rectangular waveguide. Similarly, comparison of C_2 and C_4 outputs will enable loop mismatches to be detected. Phase modulation by $\pi/2$ will permit the orthogonal components of a reflected wave to be cancelled sequentially. It will also be necessary to phase the klystron drive for maximum beam acceleration. This is done by comparing the outputs of C_2 and the phase reference cavity, first with the klystron off (so that only beam-induced signals reach the phase bridge), and then with the klystron on. The klystron drive is adjusted so that, when it is switched on, the phase of the output of C_2 changes by π.

The superconducting materials being investigated are lead, niobium and technetium. All rf experiments to date have been low-power Q measurements in TE_{011} cavities at S, C, and X-band frequencies. Work on lead is being discontinued because its soft, easily oxidized surfaces make it an unreliable material.

Niobium is the most promising rf superconductor, and cavities of very pure metal, electron-beam melted, rolled and annealed, are being machined. It is known that very high Q values can be obtained only after etching the completed parts and firing them in an ultra-high vacuum at 1900 to 2100°C. These techniques have not yet been optimized at SLAC, and the best Q obtained to date is 3×10^8. The cavity under test is suspended by a waveguide probe in a helium-filled dewar, and the Q is measured by observing the decrement of the power radiated from the cavity when the excitation is removed.

As mentioned above, the material used to construct a superconducting accelerator must withstand the presence of very high rf magnetic and electric fields. Rf losses increase rapidly when a critical magnetic field is exceeded. Similarly, field emission of electrons can take place when very high rf electric fields are present. These electrons dissipate power in the cavity walls. High power limitations imposed by these effects will be studied.

Finally, the processing difficulties experienced with niobium have encouraged the development of plating techniques for the reactor-produced element, technetium. A copper X-band TE_{011} cavity has been plated to a mirror finish, but the first rf tests were inconclusive. The work is continuing.

REFERENCES

1. R. Helm and G. A. Loew, "Beam Breakup," Linear Accelerators, edited by P. M. Lapostolle and A. Septier, (North-Holland Publishing Company, Amsterdam, 1969), Chapter B.1.4 (to be published).
2. W.K.H. Panofsky, "Transient Behavior of Beam Breakup," Report No. SLAC-TN-66-27, Stanford Linear Accelerator Center, Stanford, California (1966).
3. R. Helm, "Computer Study of Wave Propagation, Beam Loading and Beam Blowup in the SLAC Accelerator," Report No. SLAC-PUB-218, Stanford Linear Accelerator Center, Stanford, California (1966).
4. R. B. Neal, Selection of Basic Parameters, Section III, Feasibility Study for a Two-Mile Superconducting Accelerator (1969).

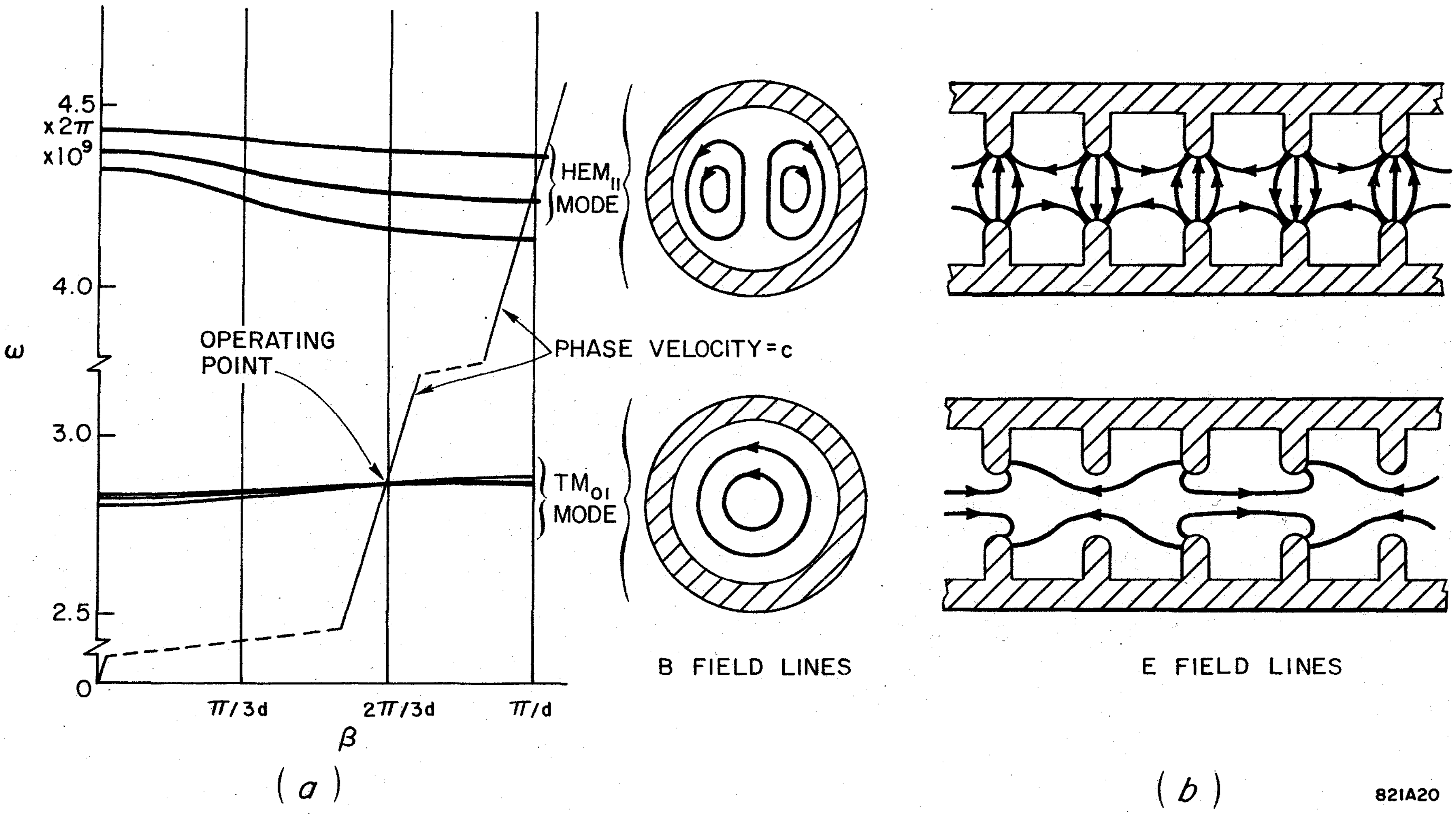

(a)

(b)

Fig. 1—(a) $\omega - \beta$ diagram of conventional disk-loaded structure.

(b) Field configuration of the HEM$_{11}$ and TM$_{01}$ modes in the disk-loaded structure.

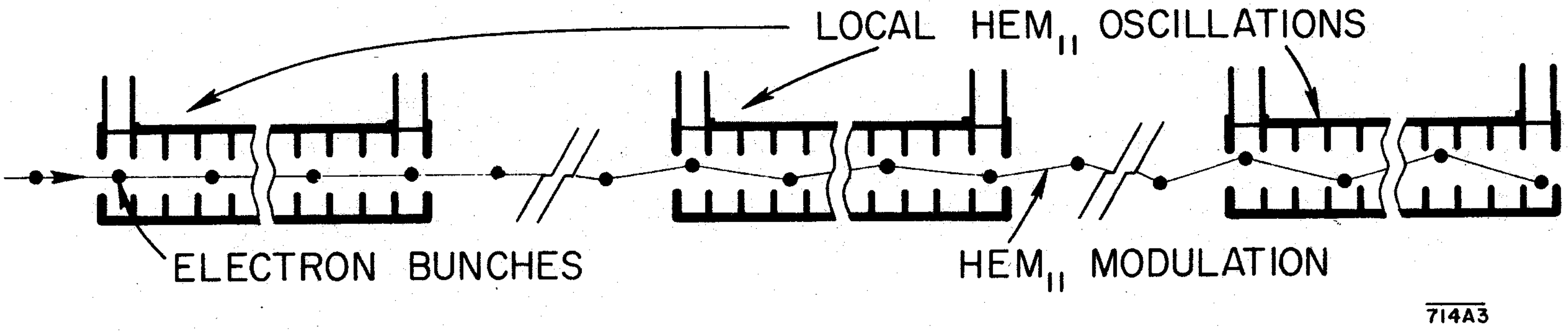

Fig. 2—Illustrating the cumulative buildup of transverse beam oscillations in a multisection accelerator.

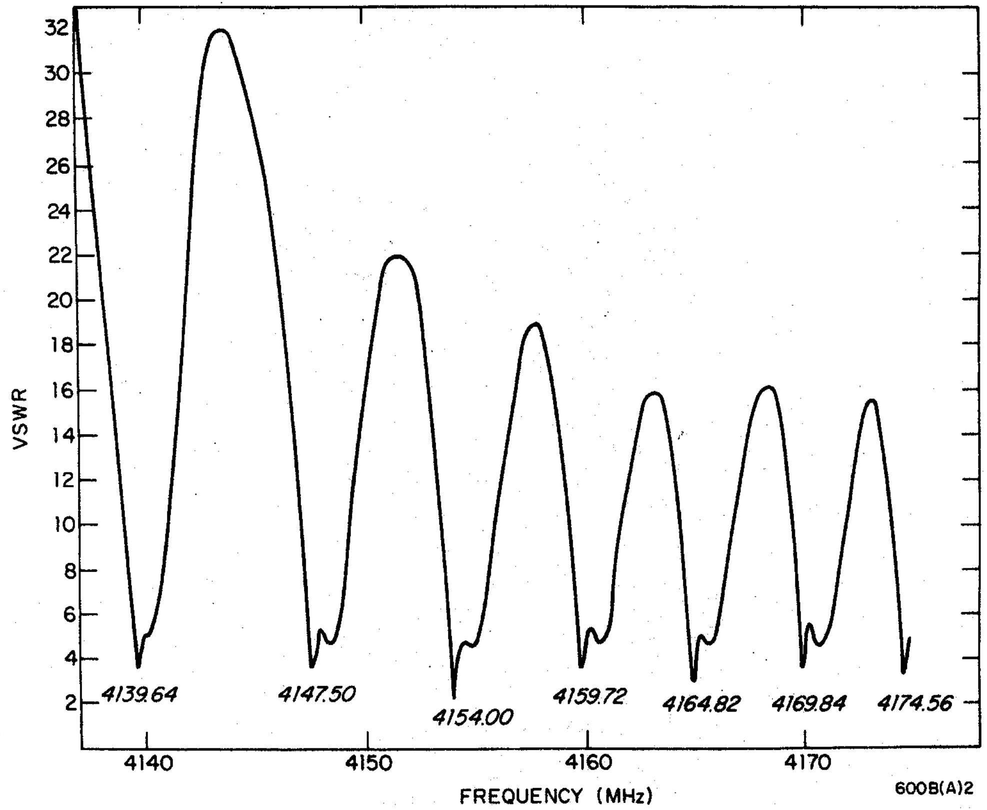

a) VSWR LOOKING INTO SECTION INPUT

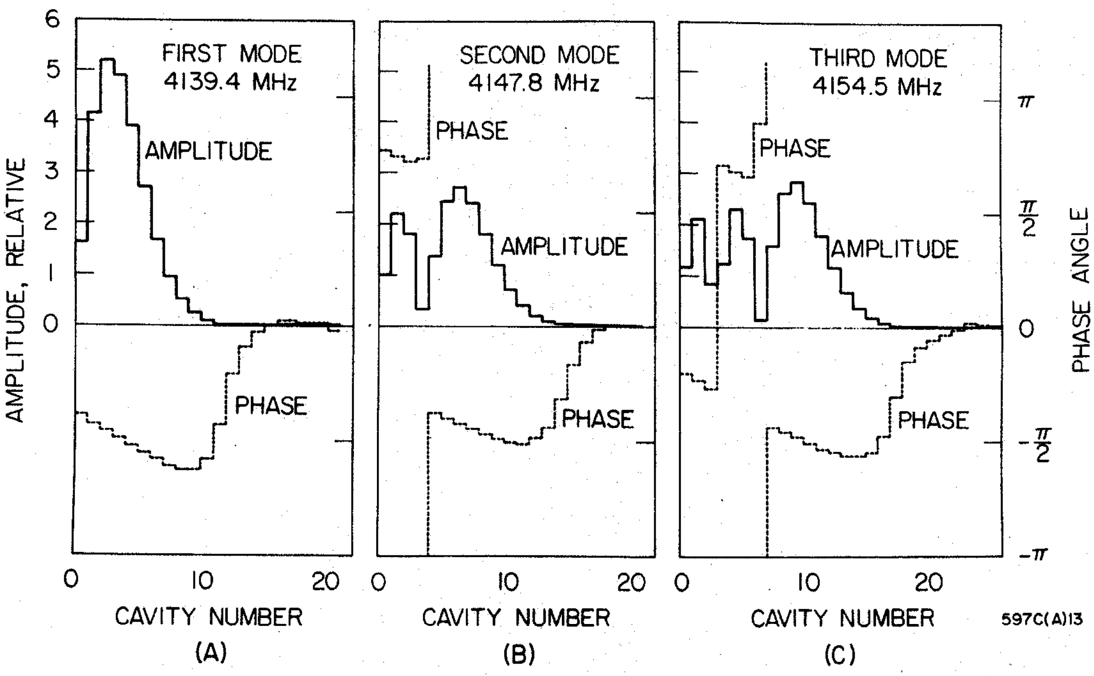

b) EXAMPLES OF COMPUTED AMPLITUDE AND PHASE DISTRIBUTION

Fig. 3 – Measured and computed HEM_{11} mode resonances in a SLAC constant-gradient section. The double dips in the measured curve are due to slight differences between the loading on horizontally - and vertically - polarized resonances.

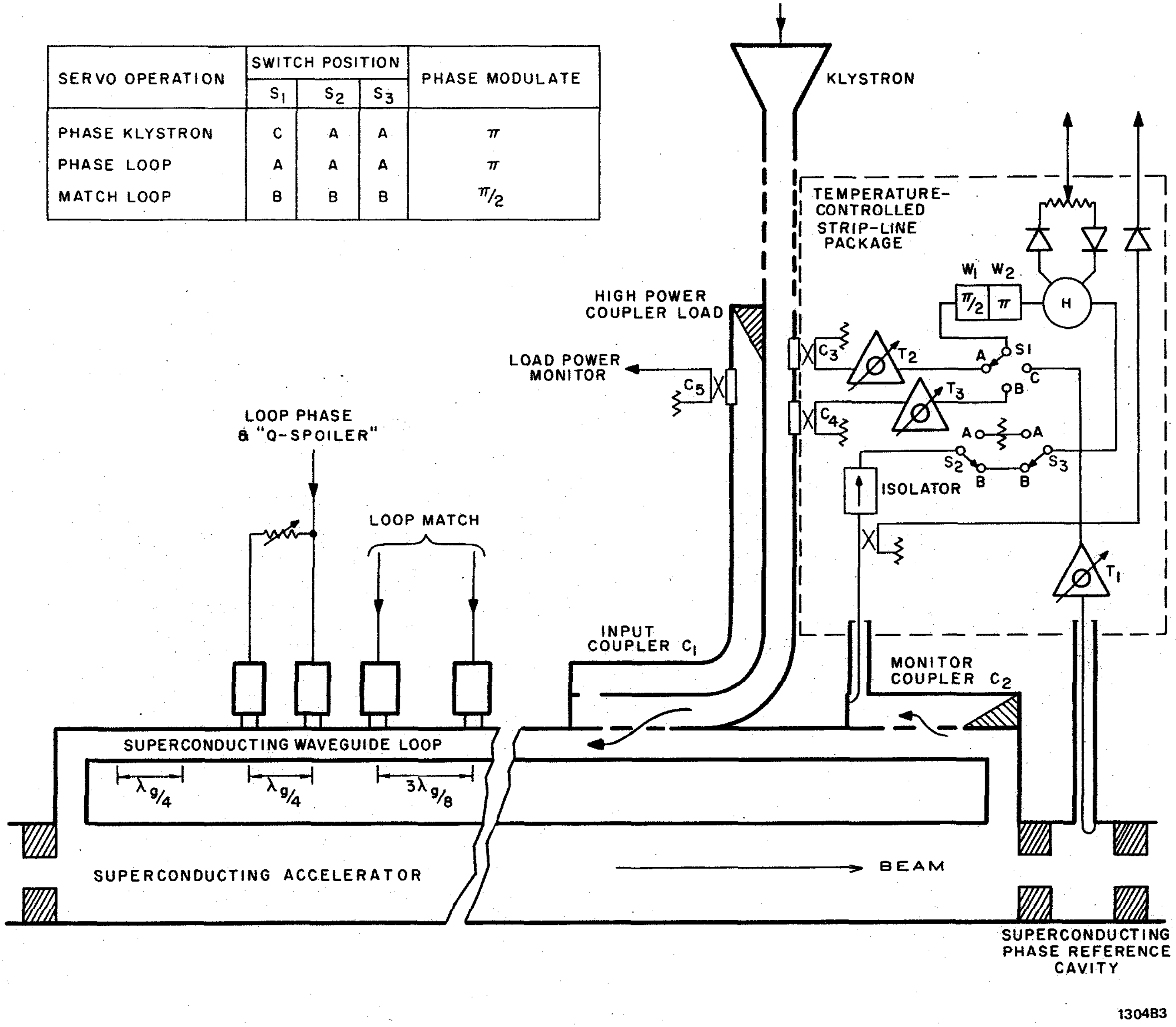

SERVO OPERATION	SWITCH POSITION			PHASE MODULATE
	S_1	S_2	S_3	
PHASE KLYSTRON	C	A	A	π
PHASE LOOP	A	A	A	π
MATCH LOOP	B	B	B	$\pi/2$

Fig. 4–Schematic diagram of a superconducting traveling-wave accelerator section with feedback, showing phasing and matching loops.

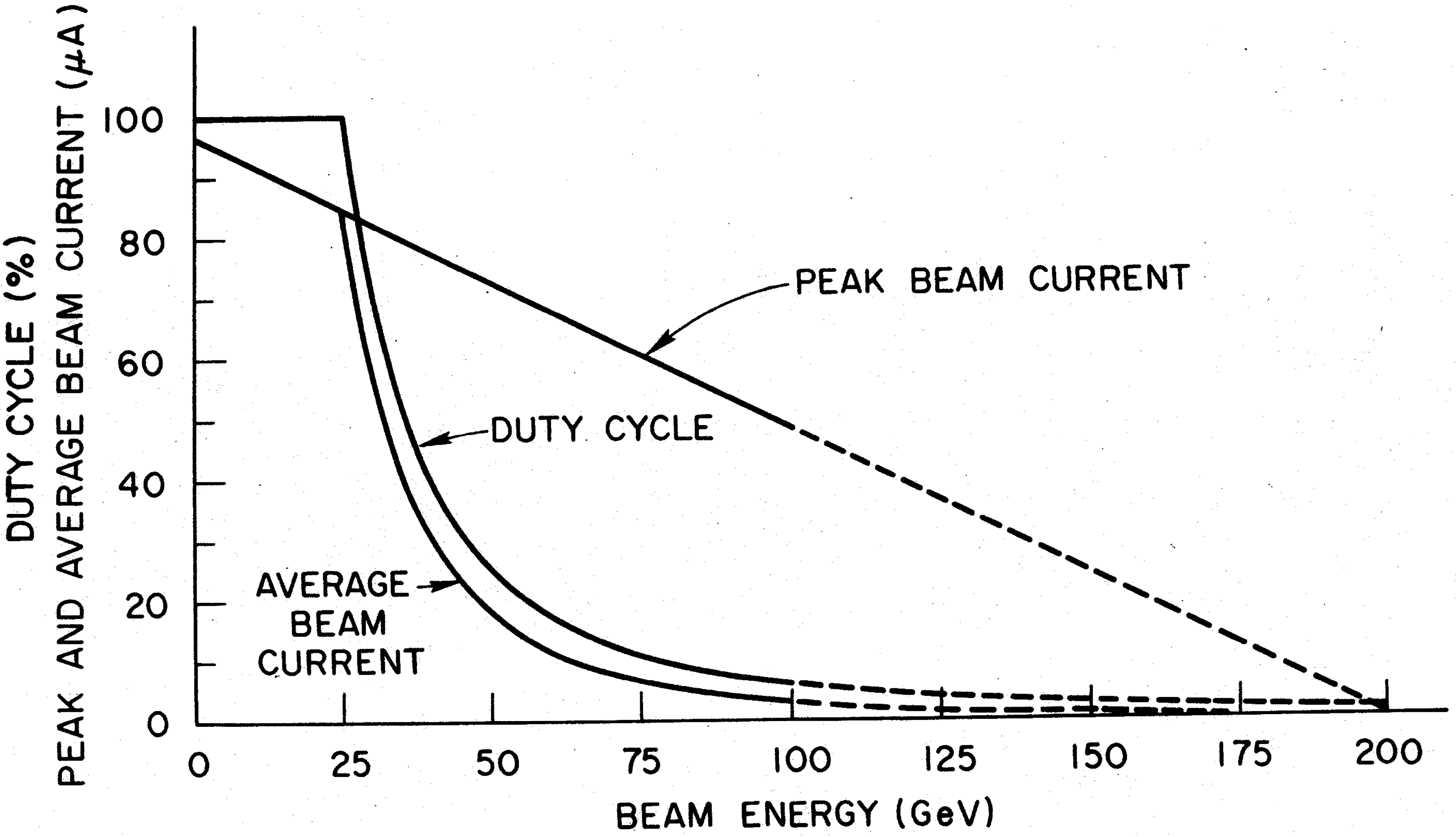

1232B3

Fig. 5–Maximum values of duty cycle, peak beam current and average beam current vs. beam energy, for the proposed superconducting linear accelerator.